



Rapidly Signal-enhanced Metabolites for Atomic Scale Monitoring of Living Cells with Magnetic Resonance

Yonghong Ding⁺,^[a, b] Sergey Korchak⁺,^[a, b] Salvatore Mamone⁺,^[a, b] Anil P. Jagtap⁺,^[a, b] Gabriele Stevanato⁺,^[a, b] Sonja Sternkopf⁺,^[a, b] Denis Moll,^[a, b] Henning Schroeder,^[a, b] Stefan Becker,^[c] André Fischer,^[d, e] Ellen Gerhardt,^[f] Tiago F. Outeiro,^[f, g, h, i] Felipe Opazo,^[b, j] Christian Griesinger,^[c, g] and Stefan Glöggler^{*,[a, b]}

Nuclear magnetic resonance (NMR) is widely applied from analytics to biomedicine although it is an inherently insensitive phenomenon. Overcoming sensitivity challenges is key to further broaden the applicability of NMR and, for example, improve medical diagnostics. Here, we present a rapid strategy to enhance the signals of ¹³C-labelled metabolites with *para*-hydrogen and, in particular, ¹³C-pyruvate, an important molecule for the energy metabolism. We succeeded to obtain an average of 27% ¹³C polarization of 1-¹³C-pyruvate in water

which allowed us to introduce two applications for studying cellular metabolism. Firstly, we demonstrate that the metabolism of 1-¹³C-pyruvate can serve as a biomarker in cellular models of Parkinson's disease and, secondly, we introduce the opportunity to combine real-time metabolic analysis with protein structure determination in the same cells. Based on the here presented results, we envision the use of our approach for future biomedical studies to detect diseases.

Introduction

Nuclear magnetic resonance (NMR) is a phenomenon that is widely used to, for example, analyze the structure of new chemicals^[1] or proteins^[2] and is even used in clinics for disease

diagnostics.^[3] Although NMR has found such a wide applicability, it is inherently insensitive. To overcome this challenge, signal-enhancement or hyperpolarization strategies have been developed, leading to amplifications of over 10,000-fold of the NMR signal.^[4–45] One key application of hyperpolarization is the

[a] Dr. Y. Ding,⁺ Dr. S. Korchak,⁺ Dr. S. Mamone,⁺ Dr. A. P. Jagtap,⁺ Dr. G. Stevanato,⁺ S. Sternkopf,⁺ D. Moll, H. Schroeder, Dr. S. Glöggler
NMR Signal Enhancement Group
Max Planck Institute for Multidisciplinary Sciences
Am Fassberg 11
37077 Göttingen (Germany)
E-mail: stefan.gloeggler@mpibpc.mpg.de

[b] Dr. Y. Ding,⁺ Dr. S. Korchak,⁺ Dr. S. Mamone,⁺ Dr. A. P. Jagtap,⁺ Dr. G. Stevanato,⁺ S. Sternkopf,⁺ D. Moll, H. Schroeder, Dr. F. Opazo, Dr. S. Glöggler
Center for Biostructural Imaging of Neurodegeneration of the University Medical Center Göttingen
Von-Siebold-Str. 3 A
37075 Göttingen (Germany)

[c] Dr. S. Becker, Prof. Dr. C. Griesinger
Department of NMR-Based Structural Biology
Max Planck Institute for Multidisciplinary Sciences
Am Fassberg 11, 37077 Göttingen (Germany)

[d] Prof. Dr. A. Fischer
Department for Epigenetics and Systems Medicine in Neurodegenerative Diseases
German Center for Neurodegenerative Diseases (DZNE)
Von-Siebold-Str. 3 A
37075 Göttingen (Germany)

[e] Prof. Dr. A. Fischer
Department of Psychiatry and Psychotherapy
University Medical Center Göttingen
Von-Siebold-Str. 5
37075 Göttingen (Germany)

[f] Dr. E. Gerhardt, Prof. Dr. T. F. Outeiro
Department of Experimental Neurodegeneration
Center for Biostructural Imaging of Neurodegeneration
University Medical Center
Waldweg 33
37073 Göttingen (Germany)

[g] Prof. Dr. T. F. Outeiro, Prof. Dr. C. Griesinger
Cluster of Excellence "Multiscale Bioimaging: From Molecular Machines to Networks of Excitable Cells" (MBExC)
University of Göttingen
37075 Göttingen (Germany)

[h] Prof. Dr. T. F. Outeiro
Max Planck Institute for Multidisciplinary Sciences
Hermann-Rein-Str. 3
37075 Göttingen (Germany)

[i] Prof. Dr. T. F. Outeiro
Translational and Clinical Research Institute
Faculty of Medical Sciences
Newcastle University
NE1 7RU Newcastle upon Tyne (UK)

[j] Dr. F. Opazo
Institute of Neuro- and Sensory Physiology
University Medical Center Göttingen
37073 Göttingen (Germany)

[*] These authors contributed equally to this work, names are listed in alphabetical order.



Supporting information for this article is available on the WWW under <https://doi.org/10.1002/cmt.202200023>



This article belongs to a Joint Special Collection dedicated to Ulf Diederichsen.



© 2022 The Authors. Published by Wiley-VCH GmbH. This is an open access article under the terms of the Creative Commons Attribution Non-Commercial License, which permits use, distribution and reproduction in any medium, provided the original work is properly cited and is not used for commercial purposes.

real-time detection of metabolic conversion allowing to probe metabolic dysfunction in, for example, cancer.^[4–8] The metabolite that is used the most for metabolic studies is $1\text{-}^{13}\text{C}$ -enriched pyruvate which is even in clinical trials as a disease marker for cancer in magnetic resonance imaging studies.^[7] The most prominent hyperpolarization technique is dissolution DNP (dynamic nuclear polarization), which is, however, only available to a few sites due to its high instrumentation complexity, high costs, and the production of hyperpolarized compounds takes long times (tens of minutes to hours).^[4–13] *Para*-hydrogen-based techniques promise to be a solution for the fast (seconds) production of hyperpolarized compounds in easy-to-use devices that can also be mobile.^[14–31] To obtain enhanced and ^{13}C -labelled metabolites such as pyruvate, *para*-hydrogen is reacted with an unsaturated metabolite precursor, the polarization is subsequently transferred to a ^{13}C atom of interest in the metabolite, followed by rapid conversion of the precursor into the desired metabolite.^[21] So far, pyruvate could only be obtained with *para*-hydrogen enhancement strategies at polarization levels below 10% in water,^[21,22] which is considered as the threshold for in vivo studies.^[27] First metabolic in vivo and cell studies have been carried out with this approach.^[22,44] As an alternative *para*-hydrogen method, the signal amplification by reversible exchange (SABRE) is extensively researched,^[32–43] but has so far only delivered highly enhanced metabolites limited to organic solvents. Most recently, up to 10% polarization of $1\text{-}^{13}\text{C}$ -pyruvate in methanol was achieved, and the approach has not yet been applied to biological studies.^[42,43]

Here, we demonstrate a strategy that allowed us to successfully obtain large degrees of polarization of various labelled forms of pyruvate in water. In particular, $1\text{-}^{13}\text{C}$ pyruvate is enhanced to 27% ^{13}C polarization on average. With such large signal enhancements, we carried out studies on a cell model for Parkinson's diseases and could show that metabolic changes can be observed with our hyperpolarized probes. Additionally, we propose here and introduce a protocol to combine hyperpolarization as real-time metabolic readout in connection with in-cell NMR^[46–51] experiments to potentially determine structural parameters of proteins and their impact on metabolic changes.

Results and Discussion

The overall concept of our study is presented in Figure 1. Here, the right column shows the hyperpolarized metabolite preparation with *para*-hydrogen as explained above for use in cell studies and potential in vivo imaging experiments. The left column demonstrates the in-cell NMR preparation that will be used together with hyperpolarization for real-time cell monitoring. For the latter, isotopically labelled proteins are brought into the living cells using electroporation. After cell recovery, the living cells can be used for structural NMR studies of proteins, and hyperpolarization is used as a real-time metabolic readout.

With a view on efficiently enhancing metabolite signals with *para*-hydrogen, three elements need to be considered and

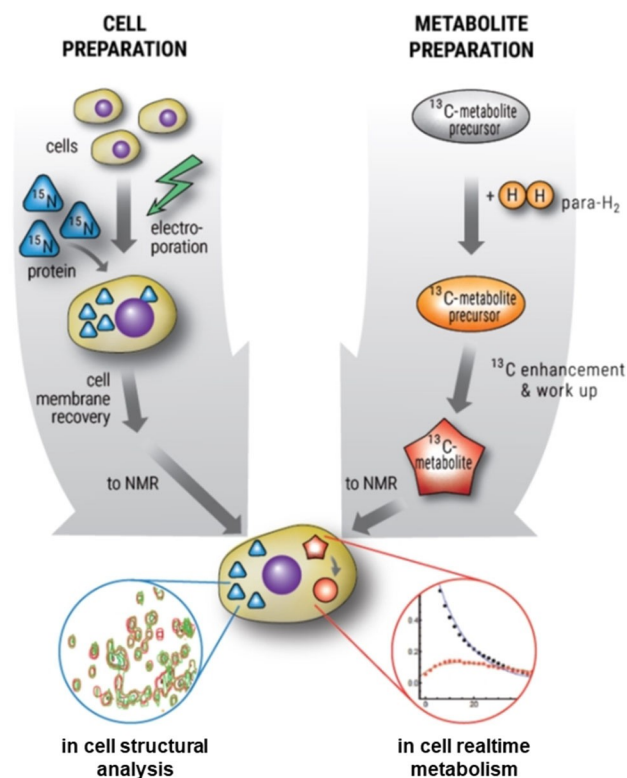
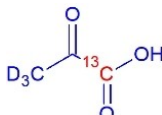
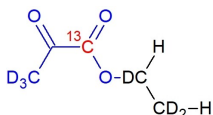
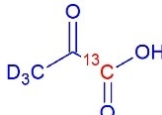
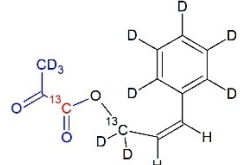
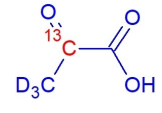
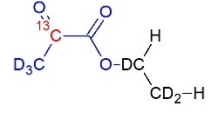
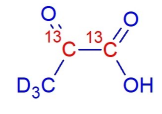
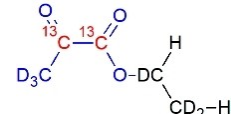

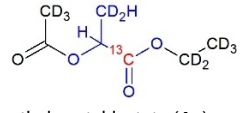


Figure 1. Concept to study protein structure and real-time cell metabolism in cells on an atomic-scale. Left: preparation of cells with isotopically enriched proteins. Right: Enhancement of ^{13}C -enriched metabolites within seconds for the read-out of the metabolism. *Para*-hydrogen (*para*- H_2) is used as the source to give enhanced proton signals (yellow) that are converted into enhanced ^{13}C signals (red) of the metabolites

optimized: 1) the precursor to which *para*-hydrogen is added, 2) the polarization transfer scheme to convert *para*-hydrogen spin order into ^{13}C polarization, and 3) the purification. Here, we have succeeded in synthesizing optimized ^{13}C precursors for pyruvate that allow us to maximize the obtainable polarization. In addition, we report on a new magnetic resonance procedure that allows to obtain largely enhanced ^{13}C metabolites. To accomplish this in a most efficient manner for a wide variety of molecules, we describe a new pulsed magnetic resonance approach (see Supporting Information) for which we propose the acronym MINERVA (Maximizing Insensitive Nuclei Enhancement Reached Via *para*-hydrogen Amplification). The MINERVA sequence allows, using hard pulses, to achieve more than 80% theoretical spin order transfer for three-spin systems consisting of two *para*-hydrogen-enhanced protons and one heteronucleus in the weak coupling regime. The only exception is when the two couplings of the protons to the heteronucleus are equal, which leads to a reduction in efficiency to 50%. As we are using hard pulses for the MINERVA sequence, a homogeneous field is not necessary for the polarization transfer. Due to the larger addressable amount of coupling networks, this sequence is more versatile than our recently published ESOTHERIC method. Our results regarding the enhancement of different ^{13}C nuclei within the metabolites pyruvate and lactate are listed in Table 1. Especially for $1\text{-}^{13}\text{C}$ -enriched pyruvate, we

Table 1. Signal-enhanced metabolites (10 mM) in H₂O and their precursor with corresponding signal enhancement (ϵ) and polarization (P). Blue indicates the metabolite with the enhanced nuclear spin in red. Black indicates the protection group/side arm that is being cleaved.

Metabolite	ϵ (B0 = 7 T)	P (13 C)	Precursor	ϵ (B0 = 7 T)	P (13 C)
 $1\text{-}^{13}\text{C}$ -pyruvate (1)	49200 ± 1800	$27 \pm 1 \%$	 ethyl pyruvate (1 a)	109000 ± 5000	$59.7 \pm 2.5 \%$
 $1\text{-}^{13}\text{C}$ -pyruvate (1)	15700 ± 1300	$8.6 \pm 0.7 \%$	 cinnamyl pyruvate (1 a')	31700 ± 1100	$17.4 \pm 0.6 \%$
 $2\text{-}^{13}\text{C}$ -pyruvate (2)	7100 ± 700	$3.9 \pm 0.4 \%$	 ethyl pyruvate (2 a)	19500 ± 1300	$10.7 \pm 0.7 \%$
 $1,2\text{-}^{13}\text{C}$ -pyruvate (3)	$2 \times ^{13}\text{C}$ 13500 ± 1800 & 11800 ± 700	$2 \times ^{13}\text{C}$ $-7.4 \pm 1.0 \%$ & $+6.5 \pm 0.4 \%$	 ethyl pyruvate (3 a)	$2 \times ^{13}\text{C}$ 42800 ± 2900 & 44400 ± 700	$2 \times ^{13}\text{C}$ $-23.5 \pm 1.6 \%$ & $+24.4 \pm 0.4 \%$
 $1\text{-}^{13}\text{C}$ -DL-lactate (4)	18800 ± 3600	$10.3 \pm 2.0 \%$	 ethyl acetyl lactate (4 a)	55200 ± 4000	$30.3 \pm 2.2 \%$

achieve $27 \pm 1\%$ ^{13}C -polarization (up to 50,000-fold signal-enhancement compared to the normal/thermally polarized signal at $B_0 = 7\text{ T}$). All of the precursors were fully hydrogenated and the procedure was optimized for full cleavage. The steps that lead us to obtain such a large polarization is due to the combination of the optimized pulse sequence, the chemistry strategy to obtain deuterated precursors, and our approach to deliver aqueous solutions of pyruvate. With respect to the deuteration, the longitudinal relaxation times of the signal-enhanced protons originating from *para*-hydrogen are larger than 100 s (see Supporting Information for details on the compounds). Such a large time reduces relaxation effects during the hydrogenation and spin order transfer. Furthermore, there are no additional spectator spins in the fully deuterated molecules that would need to be decoupled, which could otherwise interfere with the pulsed transfer of polarization. Briefly, the hyperpolarization experiments are conducted in acetone, and upon completion of the spin order transfer, a basic cleavage solution is added. Acetone, which does not form an azeotrope with water, is afterwards removed by evaporation, for example, with a high vacuum pump. After this step, we did not observe any residual acetone signal and thus make the conservative estimate that less than 1 μL could still be present in the aqueous solution. During this evaporation step, the catalyst precipitates as it is insoluble in water.

For the conducted biological studies, it is then enough to adjust for the desired pH and push the aqueous solutions through a filter (e.g., a 0.2 μm sterile filter) to obtain a solution with residual rhodium content of $17 \pm 5 \mu\text{M}$ that did not show influence on the cell viability (see Supporting Information). With a view on in vivo studies, this rhodium content is considered orders of magnitudes lower than the LD₅₀ value for rodents of several rhodium complexes.^[22]

Furthermore, we demonstrate that, with our MINERVA sequence, two ^{13}C spins can be enhanced alike within the same molecule when both ^{13}C atoms couple to each other.

Focusing on 1-¹³C-pyruvate, we were able to study the impact of α -synuclein overabundance and absence on human-derived cells in real time on metabolic rates. The protein α -synuclein has been linked to multiple systems atrophy (MSA) and Parkinson's disease whereby it is found in neurons in Lewy bodies, the characteristic pathological lesion.^[52,53] As neurodegeneration has not only been linked to proteinopathies^[52–55] but has also been connected with metabolic dysfunction,^[56–60] the interplay between protein and altered metabolism is complex, and unravelling how one affects the other promises to obtain new insights into the diseases with the ultimate goal to develop treatments. α -Synuclein has been described to play a role in mitochondrial health and metabolism.^[57,58] Pyruvate is metabolized within the mitochondria via the TCA cycle to

produce adenosine triphosphate (ATP). Under low oxygen conditions, mitochondria oxygen-independent ATP generation through the lactate dehydrogenase (LDH) is possible. However, this reaction is inefficient and produces lactate as a byproduct. High levels of lactate on affected brain regions of Parkinson's patients and the impact of α -synuclein in mitochondria function have been reported.^[61,62] Therefore, we expect that an increase of the pyruvate-to-lactate conversion can be rapidly assessed with our approach in cells that express α -synuclein in high levels when compared to cells not expressing it. To prove this hypothesis, we compared a human cell line (HEK293T) engineered to either overexpress α -synuclein with a line in which the α -synuclein gene was knocked out, thus lacking the protein (Figures 2A and B). Immunofluorescence imaging and western blot analysis confirmed the expression or absence of α -synuclein in the respective cell lines. By adding signal-enhanced pyruvate to both cell lines and observing the real-time metabolism by NMR, we monitored the pyruvate-to-lactate conversion (Figure 2C). When analyzing the metabolic rates, it became evident that the cells overexpressing α -synuclein had twice the rate of lactate production when compared to the knock-out cells.

We furthermore investigated the impact of the mitochondrial complex I inhibitor rotenone on these cells. Rotenone has been linked to the manifestation of Parkinson-like symptoms in rodents.^[63] It inhibits the aerobic mitochondrial function, which leads to higher LDH activity and, hence, to an increase of lactate production. As expected, when exposed to 2 μ M of the drug for

24 h, both cell lines showed an increased lactate production rate (Figure 2D). Mitochondria of cells overexpressing α -synuclein showed the highest observed rate.

Lastly, we introduced uniformly 15 N-isotope-labelled α -synuclein at around 5 μ M (final cellular concentration) into a human-derived cell line (HeLa) and could show that metabolism and structure can be detected in the same living cells. The results are depicted in Figure 3. First, we measured the cellular metabolism to monitor the pyruvate-to-lactate conversion (Figure 3C). Afterwards, the same cell sample was used to investigate the α -synuclein structure by 2D NMR spectroscopy.

We would like to note here, that the metabolomic experiments do not affect the downstream structural analysis (Figure S38, Supporting Information). The monomeric form of α -synuclein still remained predominant in the cell, and so did the intrinsic structural disorder, in accordance with previous findings.^[46,47] This is seen from the multiple appearing peaks in the spectrum (Figure 3A) that have not broadened due to, for example, aggregation processes. The small chemical shift differences of backbone amides between the in-cell and the disordered isolated proteins ($\Delta\delta < 0.02$ ppm) imply that cytoplasmic conditions do not induce major conformational changes. By comparison to α -synuclein in buffer, the in-cell spectrum (Figures 3A and B) revealed that major signal attenuations primarily occur to the first ten N-terminal residues, to the amino acids around Tyr39, and also to the C-terminal region, a characteristic pattern of the protein recapitulating different mammalian intracellular environments.^[44] The reduced signal intensities in these regions were proposed to partly result from the reduced mobility in the cell and also partly from weak transient hydrophobic and electrostatic interactions of N- and

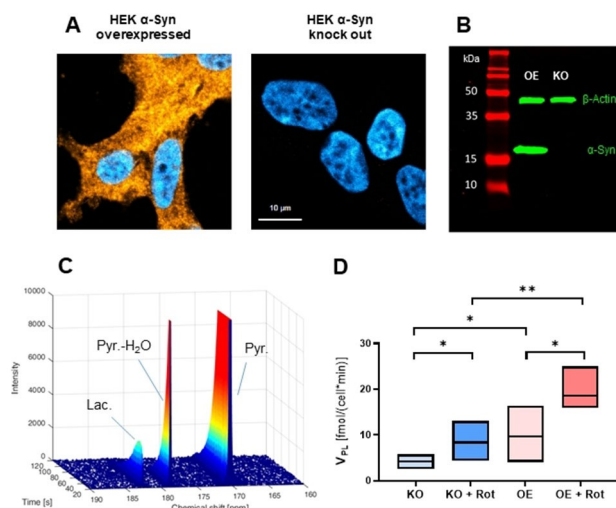


Figure 2. Signal-enhanced magnetic resonance as a biomarker for proteopathies: (A) Equally acquired and scaled confocal images of immunoassayed HEK 293T cell lines with overexpressed (OE) α -synuclein and with the α -synuclein gene knocked out (KO); cell nuclei (cyan) and α -synuclein (yellow). Scale bar: 10 μ m. (B) Western blotting of α -synuclein level of the HEK α -synuclein KO and OE cells line (kilodaltons (kDa)). (C) Series of enhanced 13 C NMR spectra acquired after perfusion of HEK cells with 1- 13 C-pyruvate. Time-dependent integrals of the signals signal were analyzed to obtain the pyruvate to lactate conversion rate (V_{PL}). (D) Box plots of V_{PL} obtained from the following conditions: α -Syn KO (n=4) and OE (n=4) without rotenone and α -Syn KO (n=6) and OE (n=4) cells with rotenone (Rot.) treatment for 24 h. Statistical significances were obtained using a one-tailed student t-test. *P < 0.05; **P < 0.01.

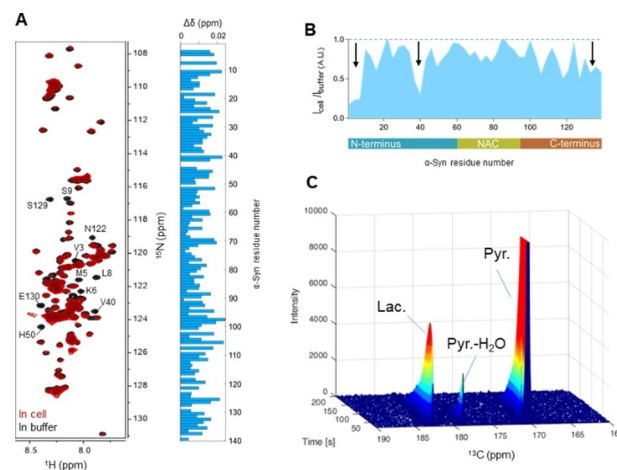


Figure 3. Atomic-scale live cell monitoring: (A) Left: overlay of ^1H - ^{15}N 2D NMR spectra of uniformly ^{15}N isotope-enriched α -Syn in HeLa Kyoto WT cells delivered through electroporation (red) and in buffer without cells (black) (representative spectra, n > 3, respectively); right: differences of their chemical shifts of non-proline backbone amides. (B) Profile of signal intensity ratio of backbone amides of α -Syn in cell to those in buffer in arbitrary units (A.U.). The ratio values are averaged among three consecutive amino acids for simplification. Arrows point to amino acid regions experiencing major signal broadening. (C) Signal-enhanced ^{13}C NMR spectra revealing the pyruvate-to-lactate conversion over 3 minutes of the same α -synuclein containing HeLa cells as in (A).

C-terminus with intracellular components. On the contrary, the signal intensities of the aggregation-prone NAC region were less affected because the region was in the center of the α -synuclein compact, shielded from exposure to the cytoplasm.^[46,47]

Conclusion

We introduced a *para*-hydrogen-based approach that allows for obtaining largely ^{13}C -enhanced metabolites within seconds. Using signal-enhanced magnetic resonance, we were able to monitor the impact of the presence of proteins such as α -synuclein related to Parkinson's disease on the metabolic function of the studied cells and, specifically here, the rate of lactate production. Additionally, we provide a combination of real-time metabolism studies and in-cell protein structure monitoring. For future studies, we are aiming at analyzing how proteins and metabolism affect each other in cells with the goal to understand onsets of diseases better. In our view, future optimization to further enhance the metabolite signals are of technical nature by, for example, developing fully automatized devices that perform the described processes. Additionally, the precursor synthesis can be optimized. We here provide a first synthetic approach to obtain deuterated $1\text{-}^{13}\text{C}$ -labelled vinyl pyruvate (single digit percent of yield) that is key to obtain largely enhanced signals; for a mass use, the yields, however, need to be significantly improved in the future.

Acknowledgements

We thank Lena Wartosch, Rebecca Gorry and Melina Schuh for access to their labs and support to perform the biochemistry experiments. Peter Lenart and his team of the live cell imaging facility, Jasmin Jakobi and Antonio Politi are acknowledged for supporting us with lab access and help to perform the biochemical studies. Furthermore, we thank Karin Giller, Melanie Wegstroth and Claudia Schwegk for the protein expression and Nikolaos Mougios for providing support for the cell imaging. For the scale-up of the precursor $1\text{a}'$, we thank Dr. Belov and the chemical synthesis facility team. We thank Hartmut Sebesse for preparing Figure 1. Lastly we thank Silvio O. Rizzoli for feedback on our work and the manuscript. The following funding sources are acknowledged: S. G. thanks the Deutsche Forschungsgemeinschaft (DFG) for funding (grants 418416679, 426677227 and 450146057). This project has received funding from the European Research Council (ERC) under the European Union's Horizon 2020 research and innovation program (Grant agreement No. 949180). T. F. O. is supported by the Deutsche Forschungsgemeinschaft (DFG, German Research Foundation) under Germany's Excellence Strategy – EXC 2067/1-390729940.

Conflict of Interest

The authors declare no conflict of interest.

Data Availability Statement

The data that support the findings of this study are available from the corresponding author upon reasonable request.

Keywords: hyperpolarization · in-cell NMR · NMR spectroscopy · *para*-hydrogen · signal enhancement

- [1] H. Günther, *NMR Spectroscopy: Basic Principles, Concepts and Applications in Chemistry*, Wiley-VCH, Weinheim, Germany 2013.
- [2] J. Cavanagh, W. J. Fairbrother, A. G. Palmer III, N. J. Skelton, *Protein NMR Spectroscopy: Principles and Practice* 2nd edn, Academic Press, 2006.
- [3] R. W. Brown, Y. C. N. Cheng, E. M. Haake, M. R. Thompson, R. Venkatesan, *Magnetic Resonance Imaging: Physical Principles and Sequence Design*, Wiley, 2014.
- [4] K. Golman, R. in't Zandt, M. Thaning, *Proc. Natl. Acad. Sci. USA* 2006, 103, 11270.
- [5] S. E. Day, M. I. Kettunen, F. A. Gallagher, D. E. Hu, M. Lerche, J. Wolber, K. Golman, J. H. Ardenkjaer-Larsen, K. M. Brindle, *Nat. Med.* 2007, 13, 1382.
- [6] F. A. Gallagher, M. I. Kettunen, S. E. Day, D. E. Hu, J. H. Ardenkjaer-Larsen, R. in't Zandt, P. R. Jensen, M. Karlsson, K. Golman, M. H. Lerche, K. M. Brindle, *Nature* 2008, 453, 940.
- [7] S. J. Nelson, J. Kurhanewicz, D. B. Vigneron, P. E. Z. Larson, A. L. Harzstark, M. Ferrone, M. van Crielinge, J. W. Chang, R. Bok, I. Park, G. Reed, L. Carvajal, E. J. Small, P. Munster, V. K. Weinberg, J. H. Ardenkjaer-Larsen, A. P. Chen, R. E. Hurd, L.-I. Odegardstuen, F. J. Robb, J. Tropp, J. A. Murray, *Sci. Transl. Med.* 2013, 198, 198ra108.
- [8] J. Kurhanewicz, D. B. Vigneron, K. Brindle, E. Y. Chekmenev, A. Comment, C. H. Cunningham, R. J. DeBerardinis, G. G. Green, M. O. Leach, S. S. Rajan, R. R. Rizi, B. D. Ross, W. S. Warren, C. R. Malloy, *Neoplasia* 2011, 13, 81.
- [9] J. H. Ardenkjaer-Larsen, B. Fridlund, A. Gram, G. Hansson, L. Hansson, M. H. Lerche, R. Servin, M. Thanning, K. Golman, *Proc. Natl. Acad. Sci. USA* 2003, 100, 10158.
- [10] P. Dzien, M. I. Kettunen, I. Marco-Ruis, E. M. Serrao, T. B. Rodrigues, T. J. Larkin, K. N. Timm, K. M. Brindle, *Magn. Reson. Med.* 2015, 73, 1733.
- [11] A. Lesage, M. Lelli, D. Gajan, M. A. Caporini, V. Vitzthum, P. Miéville, J. Alauzun, A. Roussey, C. Thieuleux, A. Mehdi, G. Bodenhausen, C. Coperet, *J. Am. Chem. Soc.* 2010, 132, 15459.
- [12] A. S. L. Thankamony, J. J. Wittmann, M. Kaushik, B. Corzilius, *Prog. Nucl. Magn. Reson. Spectrosc.* 2017, 102–103, 120.
- [13] S. Jannin, J.-N. Dumez, P. Giraudeau, D. Kurzbach, *J. Magn. Reson.* 2019, 305, 41–50.
- [14] C. R. Bowers, D. P. Weitekamp, *Phys. Rev. Lett.* 1986, 57, 2645.
- [15] A. B. Schmidt, S. Berner, W. Schimpf, C. Müller, T. Lickert, N. Schwaderlapp, S. Knecht, J. G. Skinner, A. Dost, P. Rovedo, J. Hennig, D. von Elverfeldt, J.-B. Hövener, *Nat. Commun.* 2017, 8, 14535.
- [16] P. Bhattacharya, E. Y. Chekmenev, W. H. Perman, K. C. Harris, A. P. Lin, V. A. Norton, C. T. Tan, B. D. Ross, D. P. Weitekamp, *J. Magn. Reson.* 2007, 186, 150.
- [17] P. Bhattacharya, E. Y. Chekmenev, W. F. Reynolds, S. Wagner, N. Zacharias, H. R. Chan, R. Bünger, B. D. Ross, *NMR Biomed.* 2011, 24, 1023.
- [18] M. Goldman, H. Johannesson, O. Axelsson, M. Karlsson, *C. R. Chim.* 2006, 9, 357.
- [19] T. Trantzsche, J. Bernarding, M. Plaumann, D. Lego, T. Gutmann, T. Ratajczyk, S. Dillenberger, G. Buntkowsky, J. Bargon, U. Bommerich, *Phys. Chem. Chem. Phys.* 2012, 14, 5601.
- [20] O. G. Salnikov, K. V. Kovtunov, I. V. Koptuyug, *Sci. Rep.* 2015, 5, 13930.
- [21] F. Reineri, T. Boi, S. Aime, *Nat. Commun.* 2015, 6, 5858.
- [22] E. Cavallari, C. Carrera, M. Sorge, G. Bonne, A. Muchir, S. Aime, F. Reineri, *Sci. Rep.* 2018, 8, 8366.
- [23] E. Cavallari, C. Carrera, M. Sorge, G. Bonne, A. Muchir, S. Aime, F. Reineri, *J. Magn. Reson.* 2018, 289, 12.
- [24] R. V. Shchepin, D. A. Barskiy, A. M. Coffey, I. V. Manzanera Esteve, E. Y. Chekmenev, *Angew. Chem. Int. Ed.* 2016, 55, 6071.
- [25] K. V. Kovtunov, D. A. Barskiy, R. V. Shchepin, O. G. Salnikov, I. P. Prosvirin, A. V. Bukhtiyarov, L. M. Kovtunova, V. I. Bukhtiyarov, I. V. Koptuyug, E. Y. Chekmenev, *Chem. Eur. J.* 2016, 22, 16446.
- [26] M. Haake, J. Natterer, J. Bargon, *J. Am. Chem. Soc.* 1996, 118, 8688.
- [27] S. Korchak, S. Yang, S. Mamone, S. Glöggler, *ChemistryOpen* 2018, 7, 344.

- [28] J.-B. Hövener, A. N. Pravdivtsev, B. Kidd, C. R. Bowers, S. Glöggler, K. V. Kovtunov, M. Plaumann, R. Katz-Brull, K. Buckenmaier, A. Jerschow, F. Reineri, T. Theis, R. V. Shchepin, S. Wagner, P. Bhattacharya, N. M. Zacharias, E. Y. Chekmenev, *Angew. Chem. Int. Ed.* **2018**, *57*, 11140.
- [29] S. Korchak, S. Mamone, S. Glöggler, *ChemistryOpen* **2018**, *7*, 672.
- [30] S. Korchak, A. P. Jagtap, S. Glöggler, *Chem. Sci.* **2021**, *12*, 314.
- [31] S. Knecht, J. W. Blanchard, D. Barskiy, E. Cavallari, L. Dagys, E. Van Dyke, M. Tsukanov, B. Blümel, K. Münnemann, S. Aime, F. Reineri, M. H. Levitt, G. Buntkowsky, A. Pines, P. Blümler, D. Budker, J. Eills, *Proc. Natl. Acad. Sci. USA* **2021**, *118*, e2025383118.
- [32] T. Trantzsche, J. Bernarding, M. Plaumann, D. Lego, T. Gutmann, T. Ratajczyk, S. Dillenberger, G. Buntkowsky, J. Bargon, U. Bommerich, *Phys. Chem. Chem. Phys.* **2012**, *14*, 5601.
- [33] R. W. Adams, J. A. Aguilar, K. D. Atkinson, M. J. Cowley, P. I. P. Elliott, S. B. Duckett, G. G. R. Green, I. G. Khazal, J. Lopez-Serrano, D. C. Williamson, *Science* **2009**, *323*, 1708.
- [34] P. J. Rayner, M. J. Burns, A. M. Olaru, P. Norcott, M. Fekete, G. G. R. Green, L. A. R. Highton, R. E. Mewis, S. B. Duckett, *Proc. Natl. Acad. Sci. USA* **2017**, *114*, e3188.
- [35] D. A. Barskiy, K. V. Kovtunov, I. V. Koptug, P. He, K. A. Groome, Q. A. Best, F. Shi, B. M. Goodson, R. V. Shchepin, A. M. Coffey, K. W. Waddell, E. Y. Chekmenev, *J. Am. Chem. Soc.* **2014**, *136*, 3322.
- [36] M. Suefke, S. Lehmkuhl, S. A. Liebisch, B. Blümich, S. Appelt, *Nat. Phys.* **2017**, *13*, 568.
- [37] N. Eshuis, N. Hermkens, B. J. A. van Weerdenburg, M. C. Feiters, F. P. J. T. Rutjes, S. S. Wijmenga, M. Tessari, *J. Am. Chem. Soc.* **2014**, *136*, 2695.
- [38] T. Theis, M. L. Truong, A. M. Coffey, R. V. Shchepin, K. W. Waddell, F. Shi, B. M. Goodson, W. S. Warren, E. Y. Chekmenev, *J. Am. Chem. Soc.* **2015**, *137*, 1404.
- [39] P. Spanning, I. Reile, M. Emondts, P. P. M. Schlek, N. K. J. Hermkens, N. G. J. van der Zwaluw, B. J. A. van Weerdenburg, P. Tinnemans, M. Tessari, B. Blümich, F. P. J. T. Rutjes, M. C. Feiters, *Chem. Eur. J.* **2016**, *22*, 9277.
- [40] M. L. Truong, F. Shi, P. He, B. Yuan, K. N. Plunkett, A. M. Coffey, R. V. Shchepin, D. A. Barskiy, K. V. Kovtunov, I. V. Koptug, K. W. Waddell, B. M. Goodson, E. Y. Chekmenev, *J. Phys. Chem. B* **2014**, *118*, 13882.
- [41] J. F. P. Colell, M. Emondts, A. W. J. Logan, K. Shen, J. Bae, R. V. Shchepin, G. X. Ortiz Jr., P. Spanning, Q. Wange, S. J. Malcolmson, E. Y. Chekmenev, M. C. Feiters, F. P. J. T. Rutjes, B. Blümich, T. Theis, W. S. Warren, *J. Am. Chem. Soc.* **2017**, *139*, 7761.
- [42] W. Iali, S. S. Roy, B. J. Tickner, F. Ahwal, A. J. Kennerley, S. B. Duckett, *Angew. Chem. Int. Ed.* **2019**, *58*, 10271.
- [43] P. TomHon, M. Abdulmojeed, I. Adelabu, S. Nantogma, M. S. H. Kabir, S. Lehmkuhl, E. Y. Chekmenev, T. Theis, *J. Am. Chem. Soc.* **2022**, *144*, 282.
- [44] E. Cavallari, C. Carrera, S. Aime, F. Reineri, *ChemPhysChem* **2018**, *20*, 318.
- [45] A. B. Schmidt, M. Zimmermann, S. Berner, H. de Massin, C. A. Müller, V. Ivantaev, J. Hennig, D. v. Elverfeldt, J.-B. Hövener, *Commun. Chem.* **2022**, *5*, 21.
- [46] F.-X. Theillet, A. Binolfi, B. Bekei, A. Martorana, H. M. Rose, M. Stuver, S. Verzini, D. Lorenz, M. Van Rossum, D. Goldfarb, P. Selenko, *Nature* **2016**, *530*, 45.
- [47] B. M. Burmann, J. A. Gerez, I. Matecko-Burmann, S. Campioni, P. Kumari, D. Ghosh, A. Mazur, E. E. Aspholm, D. Sulskis, M. Wawrzyniuk, T. Bock, A. Schmidt, S. G. D. Rüdiger, R. Riek, S. Hiller, *Nature* **2020**, *577*, 127.
- [48] L. Barbieri, E. Luchinat, L. Banci, *Nat. Prot.* **2016**, *11*, 1101.
- [49] E. Luchinat, L. Barbieri, M. Cremonini, L. Banci, *J. Biomol. NMR* **2021**, *75*, 97.
- [50] E. Luchinat, L. Banci, *J. Biol. Chem.* **2016**, *291*, 3776.
- [51] G. Siegal, P. Selenko, *J. Magn. Reson.* **2019**, *306*, 202.
- [52] M. G. Spillanti, M. L. Schmidt, V. M. Y. Lee, J. Q. Trojanowski, R. Jakes, M. Goedert, *Nature* **1997**, *388*, 839.
- [53] G. M. Compagnoni, A. Di Fonzo, *Acta Neuropathol. Commun.* **2019**, *7*, 113.
- [54] L. Antonschmidt, R. Dervişoğlu, V. Sant, K. T. Movellan, I. Mey, D. Riedel, C. Steinem, S. Becker, L. B. Andreas, C. Griesinger, *Sci. Adv.* **2021**, *7*, eabg2174.
- [55] G. M. Compagnoni, A. Di Fonzo, *Acta Neuropathol. Commun.* **2019**, *7*, 113.
- [56] P. J. Magistretti, I. Allaman, *Nat. Rev. Neurosci.* **2018**, *19*, 235.
- [57] S. Sarkar, M. A. Murphy, E. B. Dammer, A. L. Olson, S. Rangaraju, E. Fraenkel, M. B. Feany, *NPJ Parkinson Dis.* **2020**, *6*, 40.
- [58] D. G. Ordonez, M. K. Lee, M. B. Feany, *Neuron* **2018**, *97*, 108.
- [59] P. Borghammer, M. Chakravarty, K. Y. Jonsdottir, N. Sato, H. Matsuda, K. Ito, Y. Arahata, T. Kato, A. Gjedde, *Brain Struct. Funct.* **2010**, *214*, 303.
- [60] R. Han, J. Liang, B. Zhou, *Int. J. Mol. Sci.* **2021**, *22*, 5887.
- [61] C. Henchcliffe, M. F. Beal, *Nat. Rev. Neurol.* **2008**, *4*, 600.
- [62] A. Anandhan, M. S. Jacome, S. Lei, P. Hernandez-Franco, A. Pappa, M. I. Panayiotidis, R. Powers, R. Franco, *Brain Res. Bull.* **2017**, *133*, 12.
- [63] T. B. Sherer, R. Betarbat, C. M. Testa, B. B. Seo, J. R. Richardson, J. H. Kim, G. W. Miller, T. Yagi, A. Matsuno-Yagi, J. T. Greenamyre, *J. Neurosci.* **2003**, *23*, 10756.

Manuscript received: March 22, 2022
Version of record online: April 7, 2022